

Original Research

SLC30A2-Mediated Zinc Metabolism Modulates Gastric Cancer Progression via the Wnt/ β -Catenin Signaling Pathway

Fan Li^{1,2,†}, Xiaohong Zhang^{1,2,†}, Li Feng^{2,*}, Xingxing Zhang^{1,3,*}

Academic Editor: Alfredo Budillon

Submitted: 29 April 2024 Revised: 14 June 2024 Accepted: 19 June 2024 Published: 12 October 2024

Abstract

Background: Gastric cancer (GC) is a significant global health burden with limited treatment options. The purpose of this study was to investigate the role of SLC30A2, a zinc transporter, in GC development and its capacity as a target for therapy. Methods: A comprehensive analysis of GC datasets (GSE54129 and stomach adenocarcinoma (STAD) from The Cancer Genome Atlas (TCGA)) was conducted using bioinformatics tools to examine differential gene expression, focusing on SLC30A2. Functional assays, including Cell counting kit-8 (CCK-8) and transwell assays, were carried out on GC cell lines to determine the impact of SLC30A2 knockdown on cell behavior. Flow cytometry was utilized to quantitatively observe cell apoptosis and cell cycle progression. The impact of zinc sulfate (ZnSO₄) on GC cells was evaluated by detecting apoptosis markers, Wnt/β-catenin signaling pathway activity, and oxidative stress biomarkers, focusing on the regulatory effect of SLC30A2 overexpression. Results: Our analysis revealed significant upregulation of SLC30A2 in GC samples compared to normal samples, and high SLC30A2 expression was linked to poor prognosis. SLC30A2 knockdown repressed proliferation, invasion, and migration of GC cells, induced apoptosis, as well as arrested the cell cycle. Additionally, ZnSO₄ treatment induced cytotoxicity and oxidative stress in GC cells, while SLC30A2 overexpression rescued ZnSO₄-induced, migration, invasion, and proliferation. Moreover, ZnSO₄ had been shown to bolster apoptosis and trigger the Wnt/β-catenin signaling pathway, effects which were mitigated by the overexpression of SLC30A2. Conclusion: Our results implied that SLC30A2 was essential for GC progression by modulating zinc homeostasis and cellular processes. Targeting SLC30A2 or zinc signaling may represent a potential therapeutic approach for GC treatment.

Keywords: SLC30A2; gastric cancer; zinc metabolism; Wnt/β-catenin signaling pathway; oxidative stress; apoptosis

1. Introduction

Gastric cancer (GC), primarily presenting as stomach adenocarcinoma, accounts for over 95% of cases and is one of the most common malignant tumors globally [1]. As one of the leading contributors to cancer-related fatalities worldwide, GC exhibits high incidence and mortality rates, with an estimated 1.2 million new cases diagnosed globally annually [2]. Helicobacter pylori infection, dietary practices, alcohol intake, smoking, and genetic susceptibility are some of the variables that contribute to its etiology [3,4]. Surgery, chemotherapy, radiation therapy, and targeted therapy are the current therapeutic options for GC [5,6]. While early-stage GC can be curable with aggressive treatment, the 5-year survival rate for advanced-stage GC, even after surgical intervention, remains around 25% [7]. Recent evidence suggested that elevated serum zinc levels may have a protective role against GC. Further comprehensive research is needed to confirm these findings [8]. The urgent need for innovative diagnostic biomarkers to improve treatment outcomes and survival rates for GC patients is emphasized.

Dysregulation of the Wnt/ β -catenin signaling pathway is closely associated with almost all stages of cancer development [9]. It had been shown that transmembrane protein 64 (TMEM64) exhibits inhibition of apoptosis and enhancement of proliferation and tumorigenicity of glioma cells both in vitro and in vivo. Mechanistically, TMEM64 activates the Wnt/ β -catenin signaling pathway by accelerating the translocation of β -connexin from the cytoplasm to the nucleus, leading to an enhanced malignant phenotype of gliomas [10]. It had been found that N-acetyltransferase 10 (NAT10) promotes tumor growth and metastasis to the liver and lung. Mechanistically, NAT10 stabilises KIF23 mRNA and increases Kinesin family member 23 (KIF23) protein levels by binding to the 3'UTR region of KIF23 and increasing the N4-acetylcytidine (ac⁴C) modification of its mRNA. This activation of the Wnt/β-catenin pathway leads to an increase in the nuclear translocation of β catenin, which drives colorectal cancer (CRC) progression [11]. Disheveled3 (DVL3) enhances cancer stem cell-like (CSLC) characteristics and multidrug resistance. Through the Wnt/ β -catenin/c-Myc/SRY-box transcription factor 2

¹Fengxian District Center Hospital Graduate Student Training Base, Jinzhou Medical University, 201499 Shanghai, China

²Endoscopy Center, Minhang Hospital, Fudan University, 201199 Shanghai, China

³Department of Gastroenterology, Shanghai Jiaotong University Affiliated Sixth People Hospital South Campus, 201499 Shanghai, China

^{*}Correspondence: simonzx1989@163.com (Xingxing Zhang); feng_li@fudan.edu.cn (Li Feng)

[†]These authors contributed equally.

(SOX2) pathway, DVL3 promotes epithelial-mesenchymal transition (EMT) and CSLC traits in CRC [12]. The dysregulation of the Wnt/ β -catenin signaling pathway plays a crucial role in promoting tumor growth, metastasis, and resistance to apoptosis in various cancers.

The SLC30 family, also recognized as the Zinc Transporter (ZnT) family, comprises a set of transport proteins that are instrumental in mediating the translocation of zinc ions across cellular membranes [13]. This family includes ten members, identified as SLC30A1 through SLC30A10, playing a pivotal role in zinc homeostasis and the modulation of various cellular functions [14]. Zinc is an essential trace element in human physiology, playing a crucial role in various biological processes. Current research has concentrated on the expression patterns of *SLC30* family genes in the prognosis and therapeutic targeting within GC [15]. Analysis involving gene expression and survival data from GC patients has highlighted SLC30A5 and SLC30A7 as potential prognostic markers. Concurrently, SLC30A2 and SLC30A3 have been implicated in cancerous transformation, presenting novel avenues for therapeutic intervention [16]. SLC30A2, or ZnT2, is chiefly responsible for the regulation of intracellular and interstitial zinc ion concentrations, underscoring its importance in zinc absorption, secretion, and transport processes. The significance of SLC30A2 extends to maintaining homeostasis within the human intestinal mucosa, with genetic variations potentially impacting the susceptibility to mucosal inflammation and related intestinal pathologies [17]. The ongoing investigation into SLC30A2 aimed to elucidate the underlying mechanisms of zinc metabolism and identify new therapeutic targets for the management of GC. This research underscored the importance of the SLC30A2 transporter family in both basic and clinical research domains.

Given the critical role of SLC30A2 in zinc ion homeostasis and its emerging significance in the pathogenesis and progression of GC, this research aimed to analyze the diverse impacts of SLC30A2 expression in regulating GC progression. We aimed to elucidate the prognostic significance of SLC30A2 and its potential as a therapeutic target by integrating differential expression analysis, correlation with clinicopathological features, and functional *in vitro* assays. To understand the impacts of SLC30A2 on GC cell migration, apoptosis, invasion, and proliferation, as well as its interaction with the Wnt/ β -catenin signaling cascade in relation to zinc therapy. This study aimed to elucidate the functional mechanism of SLC30A2 in GC, potentially opening new avenues for targeted therapies to improve GC prognosis and management.

2. Material and Methods

2.1 Download of Data Sets and Screening of Differentially Expressed Genes (DEGs)

We opted for the GSE54129 dataset in the Gene Expression Omnibus (GEO) (https://www.ncbi.nlm.nih.gov/g

ds/) database, which comprised 111 human GC tissue samples and 21 non-cancerous gastric tissue samples. Furthermore, from the stomach adenocarcinoma (STAD) dataset in The Cancer Genome Atlas (TCGA) database (https://tcga-data.nci.nih.gov/tcga/), we extracted 32 adjacent non-tumor tissue samples and 375 STAD samples. The "Limma" program (version 3.6.0) in R software (version 3.6.0, R Foundation for Statistical Computing, Vienna, Austria) was used to carry out the differential expression analysis. The selection of genes was done using fold change (FC), with FC >1.3 regarded upregulated and FC <0.7 considered downregulated. a degree of significance of p < 0.05 was applied to establish statistical significance.

2.2 Assessment of SLC30A2 Expression and Correlation with Clinical Factors

To evaluate the expression levels of SLC30A2 in the GSE54129 dataset and the TCGA-STAD dataset, the Wilcoxon test was employed. Visualization of the expression data was facilitated utilizing the "ggplot2" library (version 3.2.1) within the R software. The subsequent assessment involved the application of the "survival" package (version 3.6.3) in R for conducting Kaplan-Meier (KM) survival curve analysis. This analysis aimed to assess the effects of SLC30A2 expression levels at high and low on the Progression-free Survival (PFS) probability among STAD patients, including the calculation of the log-rank pvalue. Additionally, the University of Alabama at Birmingham Cancer data analysis portal (UALCAN) database (http://ualcan.path.uab.edu/index.html) was used to study the correlation between the level of SLC30A2 and various clinical factors in TCGA-STAD samples. The clinical factors analyzed encompassed individual cancer stages, patient's gender, patient's race, tumor grade, patient's age, and lymph node metastasis status. Statistical significance threshold was specified as a p < 0.05.

2.3 Cell Culture

The Type Culture Collection of the Chinese Academy of Sciences (Shanghai, China) supplied the normal gastric mucosal cells (GES1) and the GC cell lines (AGS, HGC27, MGC803, and SNU-1). RPMI 1640 medium (Bioss, Beijing, China) was used to culture the cells. 10% fetal bovine serum (Gibco, Carlsbad, CA, USA), 100 mg/mL streptomycin (Solarbio, Beijing, China), and 100 units/mL penicillin (Gibco, Carlsbad, CA, USA) were added as supplements. All cell lines were validated by short tandem repeat (STR) profiling and tested negative for mycoplasma. Cells were all cultured in a humidified incubator at 37 °C and 5% CO₂.

2.4 Cell Transfection and Treatment

AGS and HGC27, two GC cell lines, were plated on a 24-well plate at the concentration of 2×10^5 cells each, and they were grown in full growth media for the



whole night until reaching approximately 70–80% confluence. Transfection procedures followed the manufacturer's guidelines using Lipofectamine 2000 transfection reagent (Invitrogen, Shanghai, China). Specifically, specific small interfering RNA (siRNA) targeting SLC30A2 (si-SLC30A2-1 and si-SLC30A2-2) or negative control siRNA (si-NC), as well as SLC30A2 overexpression plasmid or control vector, were transfected into GC cells. Following standardization protocols, transfections were performed in 24-well plates. Further experiments were conducted 48 hours post-transfection. To examine the impact of zinc sulfate (ZnSO₄) on GC cells, different concentrations of ZnSO₄ (10, 50, 100, 150 μ M) were administered for 24 hours post-transfection, along with saline treatment, setting the stage for subsequent analyses.

2.5 Quantitative Real-Time Polymerase Chain Reaction (qRT-PCR) Assay

Total RNA extraction from GC cells was performed utilizing the RNeasy kit (Qiagen, Beijing, China). complementary DNA (cDNA) synthesis was completed utilizing the QuantiTect SYBR Green PCR kit (Qiagen). Subsequently, the StepOnePlus real-time PCR machine (Applied Biosystems, Foster City, CA, USA) was employed to carry out qRT-PCR using the SYBR Green PCR Master Mix. For data normalization, glyceraldehyde-3-phosphate dehydrogenase (GAPDH) was utilized as an internal reference. The following primer sequences were used for amplification in **Supplementary Table 1**. Gene expression analysis was conducted using the $2^{-\Delta\Delta CT}$ method.

2.6 Western Blotting (WB) Assay

Protease and phosphatase inhibitors were included in RIPA lysis buffer (pH 8.0) (Thermo Fisher Scientific, Waltham, MA, USA) that was employed to make cell protein extracts. The bicinchoninic acid (BCA) Protein Assay Kit (Beyotime, Jiangsu, China) was employed to calculate the concentration of protein. SDS-PAGE was employed to divide equal quantities of protein, which were then deposited onto polyvinylidene fluoride (PVDF) membranes (BSA-coated, Beyotime, Jiangsu, China). Wuhan Sanying Biotechnology (Wuhan, China) provided all of the antibodies used. Primary antibodies against SLC30A2 (1:2000), Cyclin D1 (1:5000), P21 (1:1000), P27 (1:1000), Cleaved-caspase-3 (1:1000), Cleaved-caspase-9 (1:1000), Wnt-3a (1:1000), and anti- β -catenin (1:5000) were used to probe the membranes. After incubation with primary antibodies, Affinipure Donkey Anti-Goat IgG (1:3000) conjugated with horseradish peroxidase (HRP) was incubated on the membranes at room temperature for 1.5 hours, followed by visualization using the enhanced chemiluminescence (ECL) chemiluminescence detection kit (Beyotime, Jiangsu, China).

2.7 Cell Counting Kit-8 (CCK-8) Assay

Cell proliferation and viability were evaluated utilizing CCK-8 assay (CK04, Dojindo, China). In a 96-well plate, AGS and HGC27 cells were added at a cell count of 5×10^3 cells per well. Next, each well received the addition of $10~\mu L$ of CCK-8 reagent. After that, the plate was placed for four hours at 37 °C and 5% CO2. Following the incubation period, a microplate reader (Thermo Fisher Scientific, USA) was employed to measure absorbance at 450 nm. Absorbance readings were obtained at one to four days post-incubation with the CCK-8 reagent to monitor cell proliferation and generate growth curves.

2.8 Transwell Assay

Following transfection for 24 hours, cells were harvested and re-suspended at a concentration of 5×10^4 cells/well. Subsequently, these cells were inserted into the upper chambers of Transwell inserts (6-well format) covered with 10 µL of 1:9 diluted Matrigel (BD Biosciences, Shanghai, China) containing serum-free media. 600 µL of culture media with 20% fetal bovine serum (FBS, Procell, Wuhan, China) was added to the bottom chambers. The cells were then cultured for ten hours at 37 °C. The cells were fixed for 20 minutes with 4% paraformaldehyde and dyed for 30 minutes with 4',6-diamidino-2-phenylindole (DAPI). Cotton swabs were used to remove non-invaded cells from the upper surface of the membrane. The invaded cells on the lower surface were then counted and examined under a microscope. To assess cell migratory capacity, the same inserts were used without the Matrigel coating in a separate migration assay.

2.9 Flow Cytometry Analysis

To evaluate cell apoptosis and cell cycle distribution in AGS and HGC27 cells, flow cytometry analysis was performed. Initially, AGS and HGC27 cells were cultivated for 24 hours after being planted at a density of 1×10^4 cells per well in 24-well plates. Following dissociation with trypsin-Ethylenediaminetetraacetic Acid (EDTA) and washing with Phosphate Buffered Saline (PBS), cells were cultured with 5 μL of propidium iodide (PI) and 5 μL Annexin V-FITC of solution at ambient temperature for a duration of 15 minutes for apoptosis analysis. Subsequently, a flow cytometer (Jiyuan, Guangzhou, China) was used to assess the staining of PI and Annexin V, and FlowJo software version 10.4.2 (FlowJo, Ashland, OR, USA) was used to analyze the results. For cell cycle analysis, AGS and HGC27 cells were preserved for four hours at 4 °C in 75% ethanol, and thereafter stained at 37 °C for an hour with 50 µg/mL PI containing 10 mg/L RNase A. A flow cytometer (Jiyuan, Guangzhou, China) was used to assess the cell cycle distribution, and FlowJo software was applied to analyze the information.



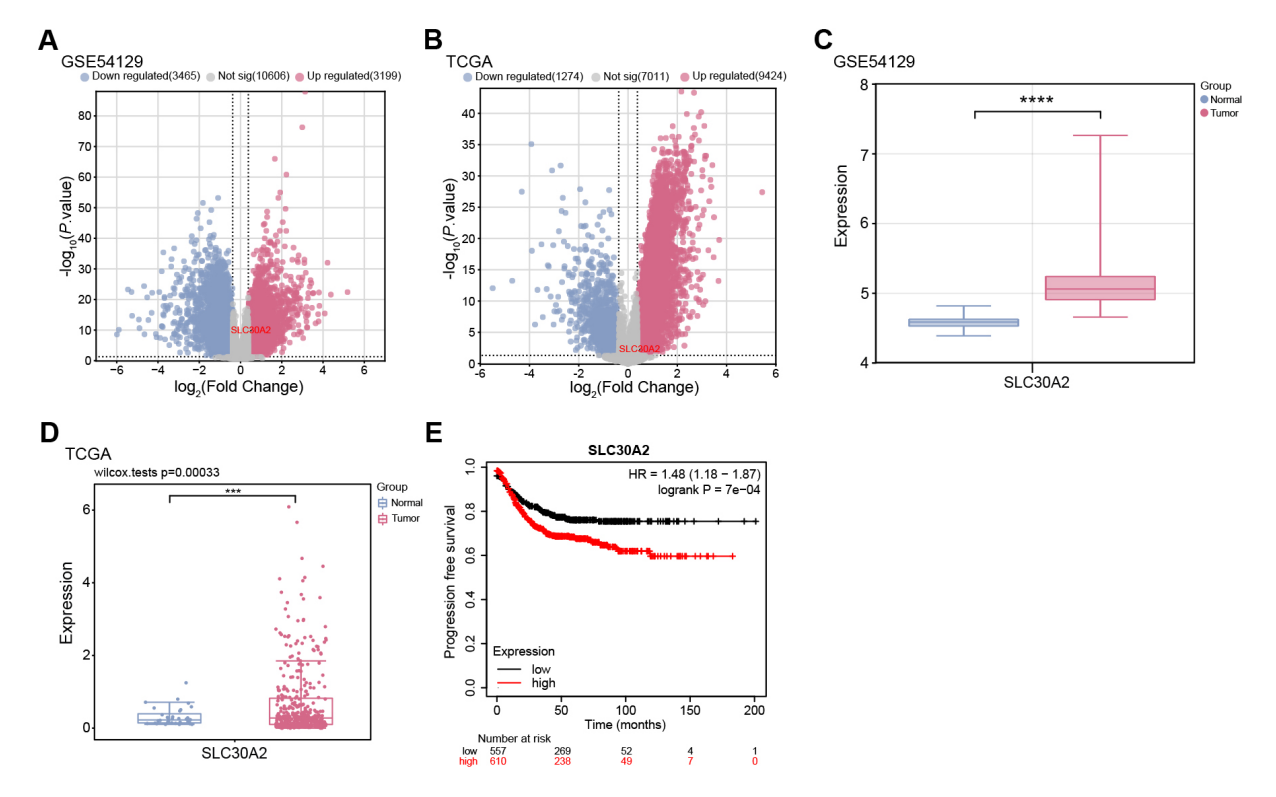


Fig. 1. Differential expression of SLC30A2 in gastric cancer (GC) and its prognostic analysis. (A,B) Volcano plot depicting the distribution of differentially expressed genes (DEGs) in the GSE54129 dataset and TCGA-STAD samples. The x-axis (Log₂ Fold Change) represents the log₂ fold change in gene expression between tumor and normal samples. The y-axis ($-\log_{10} p$ -value) indicates the statistical significance of differential expression. Up-regulated DEGs are depicted in red, and down-regulated DEGs are depicted in blue. (C,D) Box plot showing the differential expression of SLC30A2 between tumor and normal samples in the GSE54129 dataset and TCGA-STAD samples. (E) Kaplan-Meier (KM) curve demonstrating the association between SLC30A2 expression levels and Progression-free Survival (PFS) in GC patients. The abscissa represents time in months, and the ordinate is PFS probability. TCGA, The Cancer Genome Atlas; STAD, stomach adenocarcinoma. ***p < 0.001, ****p < 0.0001.

2.10 Measurement of Oxidative Stress Biomarkers

In 96-well plates, AGS and HGC27 cells were planted at a density of 1×10^4 cells per well. Following cell adherence, the monolayers were washed twice with PBS and subsequently lysed. After that, the resulting lysates were centrifuged for five minutes at 10,000 ×g to separate the supernatants. These were sonicated and utilized for the assessment of malondialdehyde (MDA), glutathione (GSH), and total oxidative stress (TOS). MDA levels, reflecting lipid peroxidation, were quantified through spectrophotometric detection of the MDA-thiobarbituric acid complex at 532 nm. The absorbance of GSH, a vital antioxidant molecule, was measured at 412 nm by its interaction with 5,5'-dithiobis (2-nitrobenzoic acid). TOS was evaluated based on oxidant-mediated conversion of ferrous to ferric ions, with the resultant color change measured at 530 nm. These assays were performed using kits from Nanjing Jiancheng Bioengineering Institute and Rel Assay (Mega Medical Co., Gaziantep, Turkey), Ensuring precise and replicable measurements of oxidative stress indicators by adhering to manufacturer protocols.

2.11 Enzyme-Linked Immunosorbent Assay (ELISA)

In this study, the secretion of Caspase-3, Cytochrome C (CYC), Tumor necrosis factor (TNF)- α , and interleukin (IL)-6 in the culture supernatants of AGS and HGC27 cells, either treated or untreated with ZnSO₄ (50 and 150 μ M, for 24 hours), was determined using ELISA kit (CUSABIO, Wuhan, China). An ELISA reader was employed to detect absorbance at 450 nm. The obtained values were compared with standard curves established using standard titration. The bicinchoninic acid (BCA) test was utilized to ascertain the protein content in each culture bottle. All concentrations were standardized to the respective cellular protein content and expressed as pg/mL (cellular protein).

2.12 Statistical Analysis

The dataset underwent statistical analysis using the R programming language. The student's t-test was utilized to analyze variations between groups and mean values along with their standard deviations (SD) were reported. An analysis of variance (ANOVA) was employed in conjunction with Tukey's post-hoc test to assess variations between several groups. p < 0.05 significance level was used.



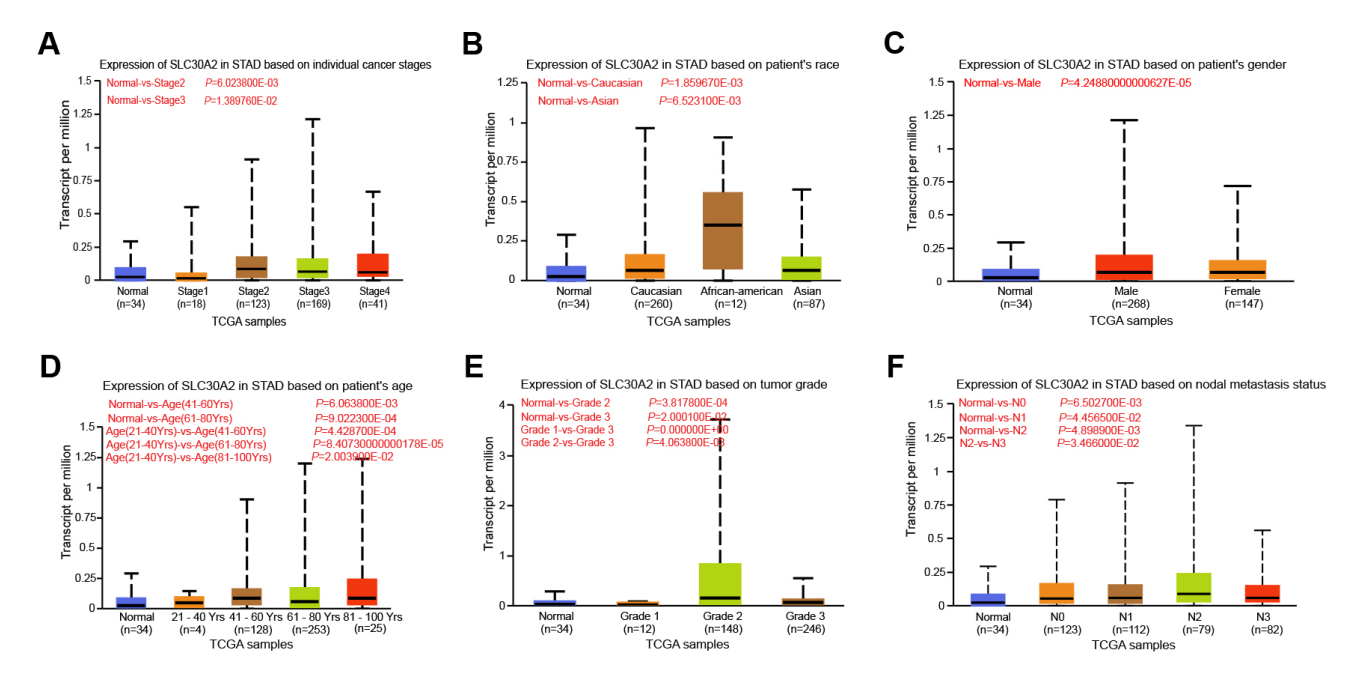


Fig. 2. Expression analysis of *SLC30A2* in UALCAN database. (A–F) Box plot illustrating the association between *SLC30A2* expression levels and individual cancer stages (A), patient's race (B), patient's gender (C), patient's age (D), tumor grades (E), and nodal metastasis statuses (F) in TCGA-STAD samples. TCGA, The Cancer Genome Atlas; STAD, stomach adenocarcinoma; UALCAN, the University of Alabama at Birmingham Cancer data analysis portal.

3. Results

3.1 Differential Expression of SLC30A2 and its Impact on the Prognosis of GC Patients

The "limma" package was employed in this work to conduct differential expression analysis on the GSE54129 dataset and TCGA-STAD samples. Specifically, 3199 upregulated DEGs and 3465 downregulated DEGs were identified from the GSE54129 dataset, while 9424 upregulated DEGs and 1274 downregulated DEGs were selected from the TCGA-STAD samples (Fig. 1A,B). Notably, SLC30A2 was identified as an upregulated gene in both the GSE54129 dataset and TCGA-STAD samples, exhibiting significant overexpression in tumor samples (Fig. 1C,D). Moreover, KM survival analysis indicated that higher expression levels of SLC30A2 were associated with a markedly reduced PFS in patients, in contrast to those exhibiting lower levels of SLC30A2 expression (p < 0.05, as shown in Fig. 1E).

3.2 Association between SLC30A2 Expression and Clinicopathological Features in TCGA-STAD

In the TCGA-STAD dataset, we examined the relationship between *SLC30A2* expression levels and different clinical-pathological factors using the UALCAN database. Our analysis indicated that *SLC30A2* expression levels were not associated with the stage of cancer (Fig. 2A), patient race (Fig. 2B), or gender (Fig. 2C). However, a significant variation in *SLC30A2* expression was observed across age groups, with the most pronounced differences being between the groups of 21–40 years and those of 41–60 years, 81–100 years, and 61–80 years (Fig. 2D). Further-

more, a clear differential expression of *SLC30A2* was noted when comparing tumor grades, with substantial variations between Grade 2 and Grade 3 tumors as well as between Grade 1 and Grade 3 tumors found (Fig. 2E). Regarding nodal metastasis status, there was a noteworthy difference in *SLC30A2* expression between cases classified as N2 and N3 (Fig. 2F).

3.3 Knockdown of SLC30A2 Suppresses Phenotypes of GC Cells in Vitro

We examined the level of SLC30A2 in GC cell lines (AGS, HGC27, MGC803, and SNU-1) and normal gastric mucosal cells (GES1). The findings demonstrated that SLC30A2 was substantially expressed in all GC cell lines compared to normal tissues, with significant upregulation observed particularly in the AGS and HGC27 cell lines (Fig. 3A-C). Therefore, these two cell lines were selected for further exploration of the functional significance of SLC30A2 in GC. Subsequently, we evaluated the transfection efficiency of SLC30A2 knockdown plasmids in AGS and HGC27 cells employing WB and qRT-PCR (Fig. 3D-G). The invasion, migration, and proliferation abilities of AGS and HGC27 cells following SLC30A2 knockdown were assessed using CCK-8 and Transwell assays (Fig. 3H-K). In comparison to the control group, the outcomes demonstrated that SLC30A2 knockdown suppressed the growth, invasion, and migration of AGS and HGC27 cells.



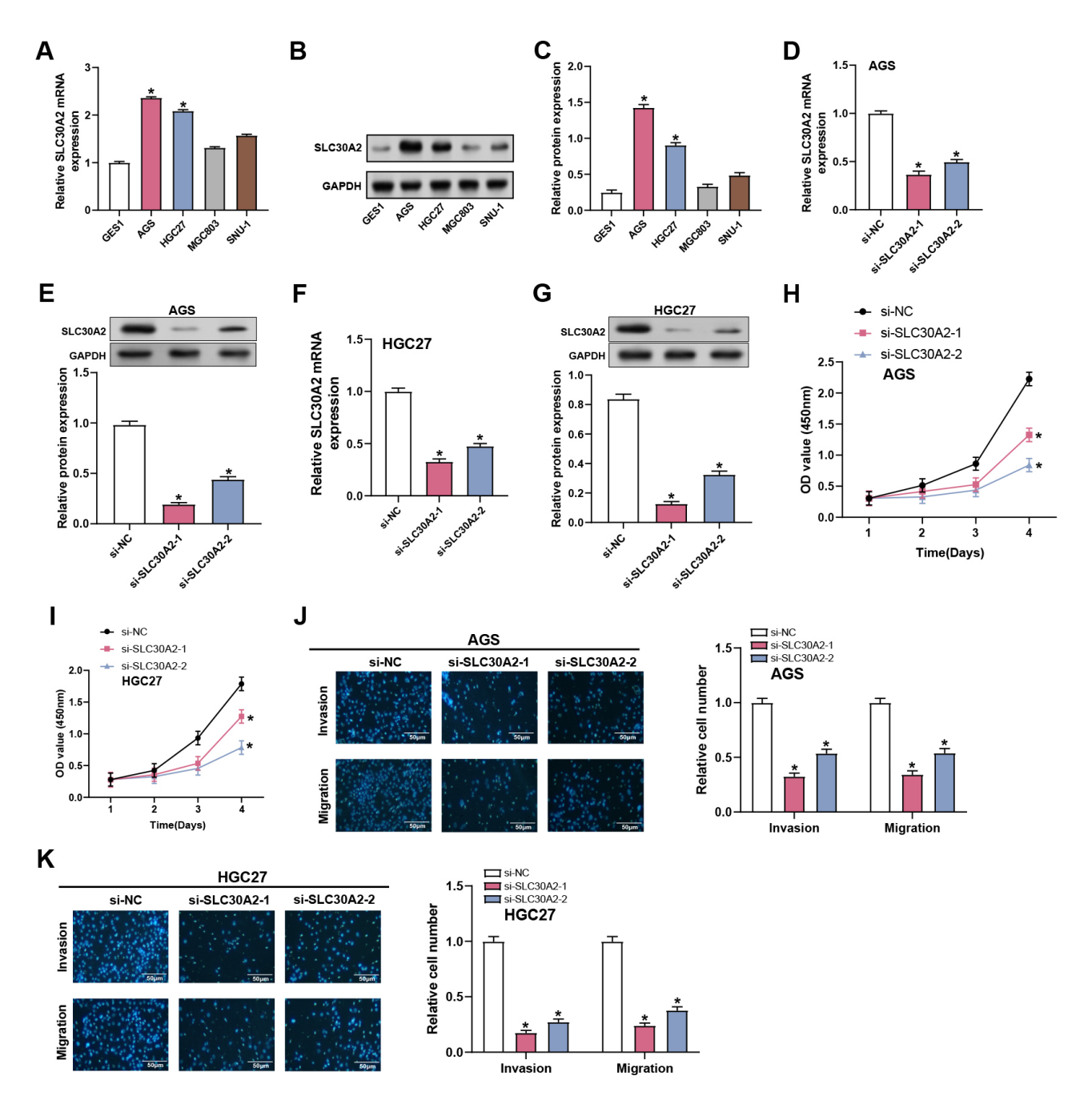


Fig. 3. Effects of SLC30A2 knockdown on GC proliferation, invasion and migration. (A–C) qRT-PCR and WB analysis depicting the mRNA and protein expression levels of SLC30A2 in normal gastric mucosal cells (GES1) and GC cell lines (AGS, HGC27, MGC803, and SNU-1). (D–G) Assessment of the transfection efficiency of SLC30A2 knockdown plasmids in AGS and HGC27 cells using qRT-PCR and WB analysis. (H,I) CCK-8 results show the proliferation abilities of AGS and HGC27 cells following SLC30A2 knockdown. (J,K) Evaluation of the invasion and migration abilities of AGS and HGC27 cells following SLC30A2 knockdown using Transwell assays. Representative images of the underside of the membrane stained with DAPI illustrate the invasion and migration of cells (left). Quantification of cell invasion and migration represented as a percentage of cell count (right). Magnification: $200\times$, scale bar = 50 μ m. qRT-PCR, Quantitative real-time polymerase chain reaction; WB, Western blotting; mRNA, messenger RNA; CCK-8, cell counting kit-8; NC, negative control. *p < 0.05.

3.4 SLC30A2 Knockdown Promotes Apoptosis and Cell Cycle Arrest in GC Cells

After SLC30A2 knockdown, flow cytometry analysis evaluated apoptosis and cell cycle distribution in AGS and

HGC27 cells. Our findings showed that *SLC30A2* knockdown enhanced apoptosis in AGS and HGC27 cells relative to the control group, along with a reduce in the proportion of cells in the S phase, indicating cell cycle arrest



during the G1 to S transition (Fig. 4A–C). Subsequently, qRT-PCR and WB assays were conducted to evaluate the gene and levels of cell cycle proteins (Cyclin D1, P21, and P27) in AGS and HGC27 cells after *SLC30A2* knockdown. Our findings revealed that *SLC30A2* knockdown resulted in a decline in Cyclin D1 expression and increased P27 and P21 expression in contrast to the control group (Fig. 4D–I). Those findings indicated that *in vitro* cell cycle arrest and apoptosis are enhanced by *SLC30A2* knockdown.

3.5 ZnSO₄ Induces Cytotoxicity and Oxidative Stress in GC Cells

The CCK-8 test was showed that at a concentration of $150~\mu M$, $ZnSO_4$ considerably decreased the viability of AGS and HGC27 cells (Fig. 5A,B). To further investigate the impact of zinc on oxidative stress in GC cells, the level of MDA, GSH, and TOS were evaluated utilizing respective assay kits in AGS and HGC27 cells subjected to 50 and $150~\mu M$ concentrations of $ZnSO_4$. The findings indicated that in contrast to the group under control, MDA and TOS levels exhibited concentration-dependent increases, while GSH levels showed concentration-dependent decreases in response to $ZnSO_4$ treatment (Fig. 5C–H). These results suggested that $ZnSO_4$ exerts cytotoxic effects and induces oxidative stress in GC cells, underscoring its potential impact on the cellular redox state and viability.

3.6 ZnSO₄ Modulates Apoptotic and Inflammatory Markers in Gastric Cancer Cell Lines

ELISA analysis results showed that exposure to ZnSO₄ significantly affected apoptosis and inflammatory biomarkers in AGS and HGC27 cell lines. After treatment with different concentrations of ZnSO₄ (50, 150 μM), a dose-dependent rise in the levels of Caspase-3 was observed in AGS (Fig. 6A) and HGC27 cells (Fig. 6B), indicating enhanced apoptotic activity. Similarly, CYC levels in AGS (Fig. 6C) and HGC27 cells (Fig. 6D) also increased with increasing ZnSO₄ concentration, further confirming the induction of apoptosis. In addition to these apoptotic markers, proinflammatory cytokines were also assessed. In GC cells, compared to the control group, TNF- α and IL-6 levels rose in a concentration-dependent way in response to ZnSO4 (Fig. 6E–H). These findings highlighted that ZnSO₄ treatment not only causes GC cells to undergo apoptosis but also promotes a pro-inflammatory environment.

3.7 Overexpression of SLC30A2 Restores ZnSO₄-Induced Proliferation, Migration, and Invasion of GC Cells

The assays of qRT-PCR and WB were employed to evaluate the effectiveness of *SLC30A2* overexpression in AGS and HGC27 cells (Fig. 7A–C). Proliferation, invasion, and migration of AGS and HGC27 cells under five different treatment conditions (control, saline, saline + ZnSO₄, saline + ZnSO₄ + Vector, and saline + ZnSO₄ + over-*SLC30A2*) were assessed using CCK-8 and Transwell as-

says (Fig. 7D–G). The control and saline groups did not significantly vary from one another, according to the results. Following the addition of ZnSO₄ to the saline group, a reduction in cell proliferation, invasion, and migration was observed. However, this inhibitory effect was partially reversed when ZnSO₄ and overexpression of *SLC30A2* were combined in the saline medium. These results indicated that *SLC30A2* is vital not only in mediating the cytotoxic response of ZnSO₄ but also in encouraging the invasion and migration properties of GC cells.

3.8 SLC30A2 Overexpression Regulates ZnSO₄-Induced GC Cell Apoptosis and Activation of the Wnt/ β -Catenin Signaling Pathway

To further elucidate the impacts of ZnSO₄ treatment and SLC30A2 overexpression on GC cell apoptosis and the Wnt/ β -catenin signaling pathway. Wnt-3a, β -catenin, cleaved caspase-3, and cleaved caspase-9 expression levels were evaluated using qRT-PCR and WB assays (Fig. 8A-L). Between the GC cell control and saline groups, there was no discernible difference in the outcomes. However, after adding ZnSO₄ to the saline group, the amounts of Cleaved caspase-3 and Cleaved caspase-9 rose, indicating that the apoptosis pathway was enhanced. Similarly, Wnt/3a and β -catenin expression levels rose, indicating that the Wnt/ β -catenin signaling pathway was triggered. Contrary to these effects, overexpression of SLC30A2 markedly mitigated the ZnSO₄-induced upregulation, leading to decreased production of Wnt-3a, β -catenin, cleaved caspase-3, and cleaved caspase-9. These findings indicated that zinc promoted GC cell apoptosis and initiates the Wnt/ β -catenin signaling pathway, and SLC30A2 overexpression can prevent this effect.

4. Discussion

GC remains a significant clinical problem, necessitating extensive molecular study and the development of novel treatment routes [18]. Zinc metabolism and homeostasis have emerged as important variables in the pathophysiology of GC [19]. Studies investigating the complicated link between dysregulated zinc homeostasis and carcinogenesis have underlined the importance of oxidative stress [20,21]. Qi J et al. [22] proposed that MCOLN1/TRPML1 regulates autophagy in various cancers by mediating lysosomal zinc release into the cytoplasm. Zinc influx triggered by MCOLN1 activation can block the autophagy pathway, impacting cell survival and death. Consequently, zinc plays a crucial role in the regulation of autophagy mediated by MCOLN1. Additionally, Zhu M et al. [23] observed that the overexpression of zinc finger protein 64 (ZFP64) in GC is associated with invasive phenotypes and resistance to nanoparticle albumin-bound paclitaxel (nab-paclitaxel), serving as an independent prognostic factor for GC. These results affirmed the essential function of zinc homeostasis in the complex progression of GC.



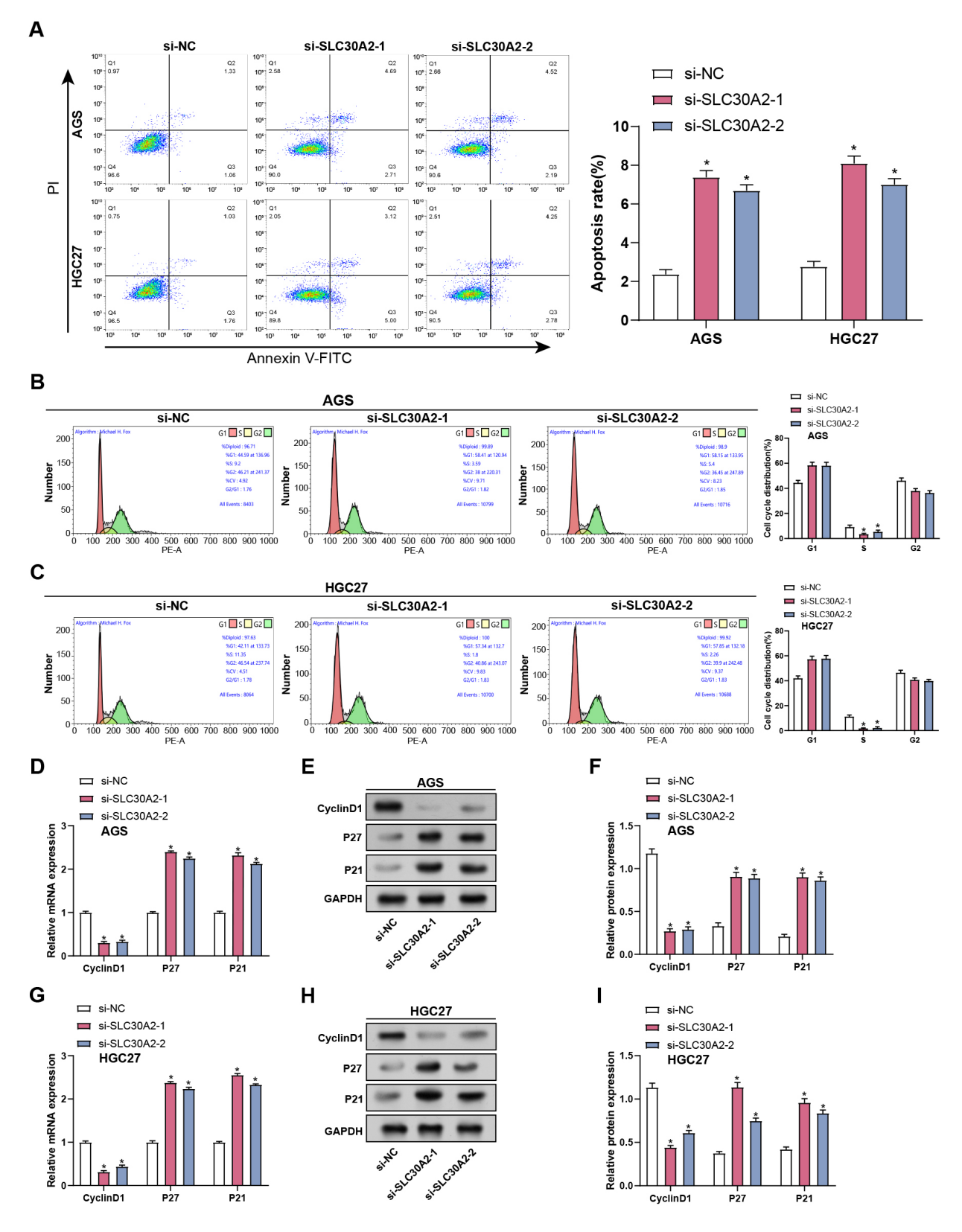


Fig. 4. Impact of SLC30A2 knockdown on apoptosis and cell cycle progression in GC cells. (A–C) Flow cytometry analysis illustrating the effects of SLC30A2 knockdown on apoptosis and cell cycle distribution in AGS and HGC27 cells. (D–I) qRT-PCR and WB analysis of the mRNA and protein expression levels of cell cycle proteins (Cyclin D1, P27, and P21) in AGS and HGC27 cells following SLC30A2 knockdown. qRT-PCR, Quantitative real-time polymerase chain reaction; WB, Western blotting; mRNA, messenger RNA. *p < 0.05.

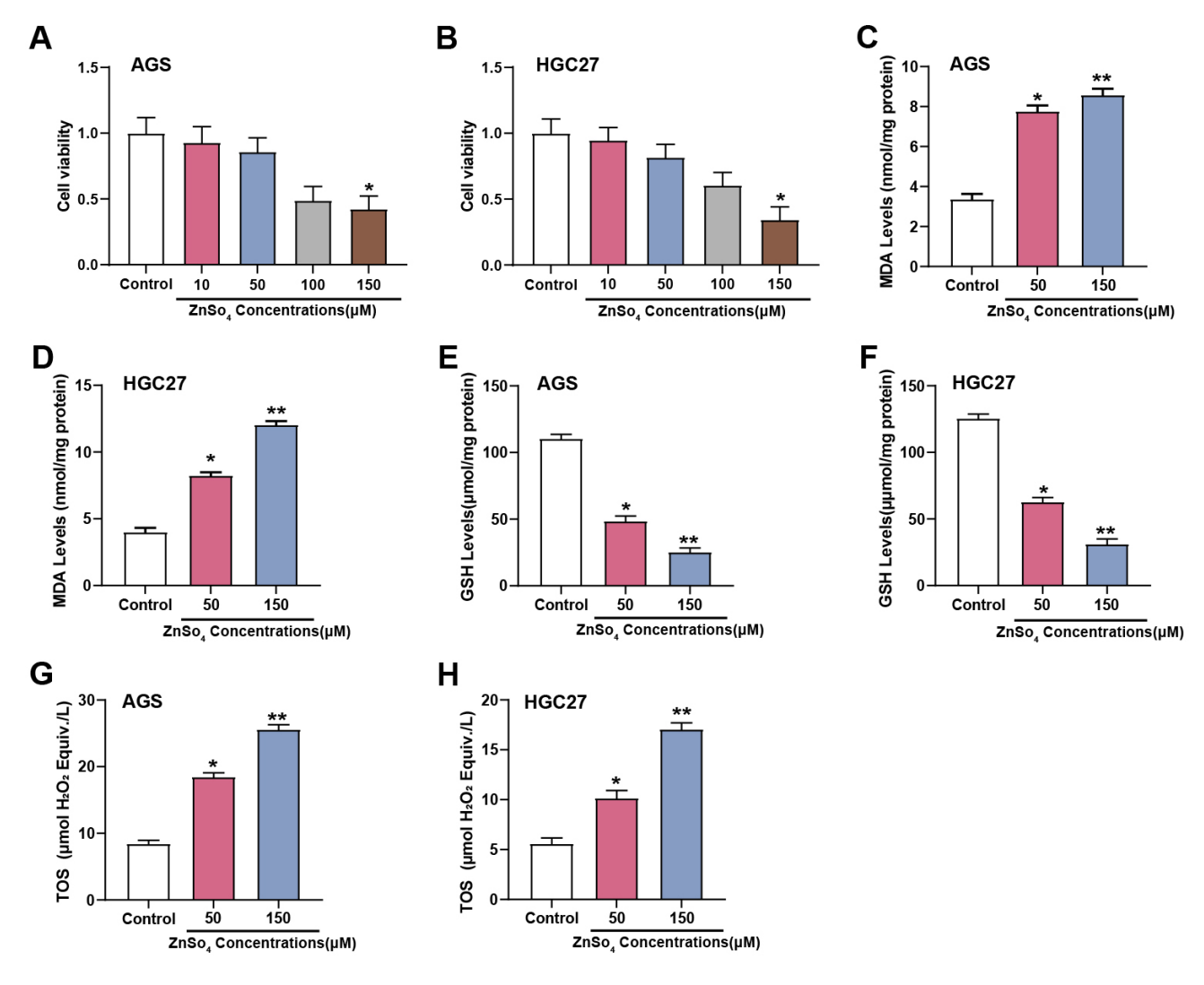


Fig. 5. Effects of ZnSO₄ on cytotoxicity and oxidative stress in GC cells. (A,B) The viability of AGS and HGC27 cells treated with different concentrations of ZnSO₄ (0, 10, 50, 100, 150 μ M) was assessed using the CCK-8 assay. The Y-axis represents cell viability, and the X-axis represents different concentrations of ZnSO₄ treatment conditions. (C–H) Measurement of MDA, GSH, and TOS levels in AGS and HGC27 cells treated with 50 and 150 μ M concentrations of ZnSO₄ using respective assay kits; CCK-8, cell counting kit-8; MDA, malondialdehyde; GSH, glutathione; TOS, total oxidant status; ZnSO₄, zinc sulfate. *p < 0.05, **p < 0.01.

The SLC30A2 gene encodes zinc transporter 2 (ZnT-2), which maintains the balance and homeostasis of intracellular zinc ions [24]. Disruption of intracellular zinc ion balance may affect immune function and diseases related to the nervous system [25,26]. Additionally, it was observed that SLC30A2 levels were down-regulated in patients with GC who had bone metastasis, indicating that SLC30A2 plays a significant role in the bone metastasis of it [27]. Furthermore, Ren X et al. [28] demonstrated that overexpression of SLC39A10 enhances the malignant characteristics of GC cells by increasing the availability of zinc ions, further promoting the activity of casein kinase 2 (CK2), activating the MAPK/ERK and PI3K/AKT pathways, and driving the malignant progression of GC. Through bioinformatic analysis of GC samples, we observed a significant increase in SLC30A2 expression in GC, correlating with disease recur-

rence, progression, patient age, lymph node metastasis, and tumor grade. Knockdown experiments demonstrated that reducing *SLC30A2* levels hindered GC cell growth, migration, and invasion, arrested the cell cycle, and promoted apoptosis. These findings highlighted *SLC30A2* as a potential therapeutic target.

Zinc is an essential trace element for human health, necessary for cellular growth and tissue repair [29,30]. Recent evidence has shown a correlation between serum zinc levels and GC localization, with a significant deficiency observed in postoperative GC patients [31]. This deficiency is closely associated with reduced serum albumin levels, indicating that elevated serum zinc may act as a protective factor against GC risk. The importance of zinc in oncology is further underscored by the therapeutic use of ZnSO₄ to create a high-zinc ion environment in various cancer cells, in-



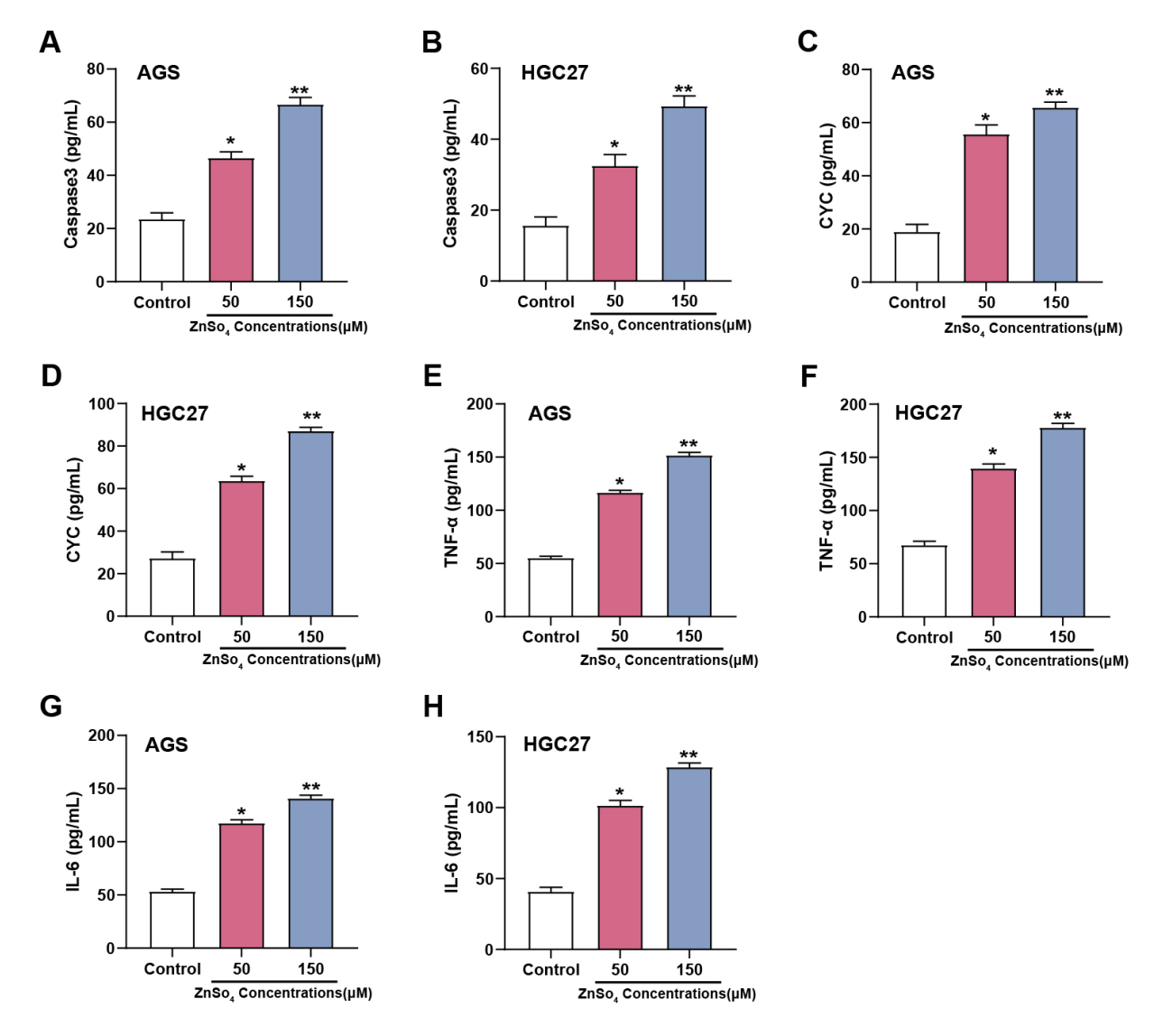


Fig. 6. ZnSO₄ modulates apoptotic and inflammatory markers in GC cells. (A–H) Expression levels of apoptotic markers Caspase3 (A,B) and CYC (C,D), as well as inflammatory cytokines Tumor necrosis factor (TNF)- α (E,F) and interleukin (IL)-6 (G,H), were evaluated by ELISA in AGS and HGC27 cells treated with 50 and 150 μ M concentrations of ZnSO₄. The Y-axis represents the expression level of each marker, and the X-axis represents different treatment conditions with ZnSO₄. CYC, cytochrome C; ZnSO₄, zinc sulfate; ELISA, Enzyme-Linked Immunosorbent Assay. *p < 0.05, **p < 0.01.

cluding those of prostate cancer and osteosarcoma [32,33]. The interplay between oxidative stress and cancer progression is underscored by findings from Jelić MD *et al.* [34], revealing lower antioxidant enzyme levels and higher 8-hydroxy-2'-deoxyguanosine (8-OHdG) and MDA concentrations across different cancers. This correlation signifies oxidative stress as a pivotal factor in oncogenesis. Specifically, Wang S *et al.* [35] demonstrated that *PRDX2* knockdown amplifies oxidative stress in response to Helicobacter pylori infection and increases GC cell sensitivity to cisplatin, illustrating the impact of oxidative mechanisms in GC pathophysiology. Lin JX *et al.* [36] further investigated systemic inflammatory responses (SIR) in GC patients, finding that postoperative lymphocyte-monocyte ratio (LMR) can predict long-term survival, thereby linking

inflammation with GC outcomes. Inflammation, a driving force behind the tumor microenvironment (TME) and GC occurrence, suggests targeting TME components as a viable strategy for GC management. The contribution of inflammation to the TME and its role in GC onset was highlighted by Rihawi K *et al.* [37], pointing to the tumor-promoting effects of inflammatory processes. Our experiments investigated the effects of ZnSO₄ treatment on oxidative stress markers (MDA, TOS, and GSH) in GC cells, revealing an increase in MDA and TOS levels and a decrease in GSH levels, indicating induction of oxidative stress. Additionally, ZnSO₄ treatment led to a significant reduction in GC cell viability, accompanied by elevated levels of apoptosis-related proteins (Caspase-3 and CYC) and inflammatory markers (TNF-α and IL-6), suggesting a potential influ-



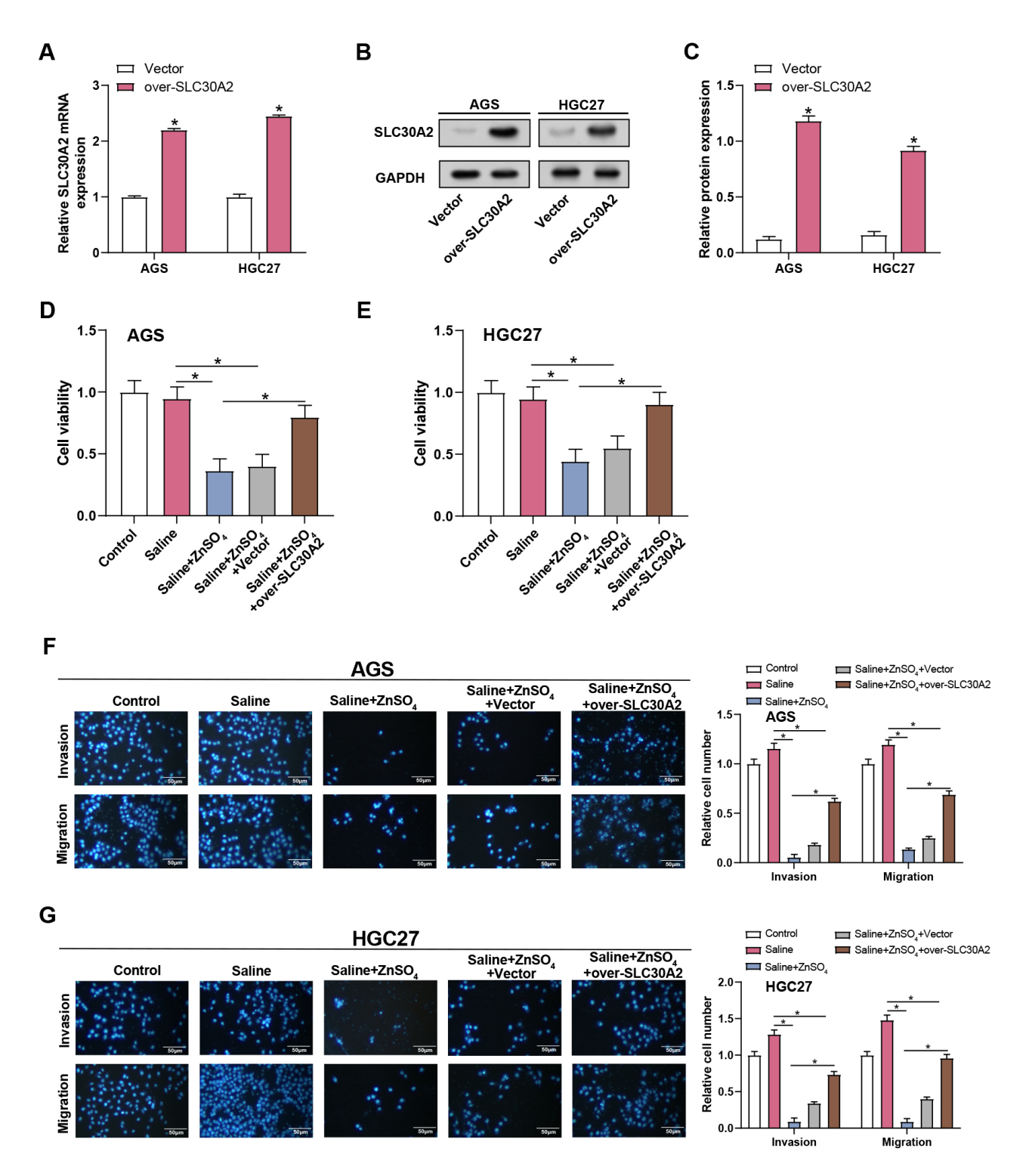


Fig. 7. Overexpression of SLC30A2 rescues $ZnSO_4$ -induced inhibition of proliferation, invasion, and migration in GC cells. (A–C) The efficiency of SLC30A2 overexpression in AGS and HGC27 cells was assessed by qRT-PCR and WB assays. (D–G) Proliferation, invasion, and migration of AGS and HGC27 cells under different treatment conditions (control, saline, saline + $ZnSO_4$, saline + $ZnSO_4$ evaluated by CCK-8 (D,E) along with Transwell assays (F,G). Representative images of the underside of the membrane stained with DAPI illustrate the invasion and migration of cells (left). Quantification of cell invasion and migration represented as a percentage of cell count (right). Magnification: $200\times$, scale bar = $50 \mu m$. qRT-PCR, Quantitative real-time polymerase chain reaction; WB, Western blotting; CCK-8, cell counting kit-8; $ZnSO_4$, zinc sulfate. *p < 0.05.

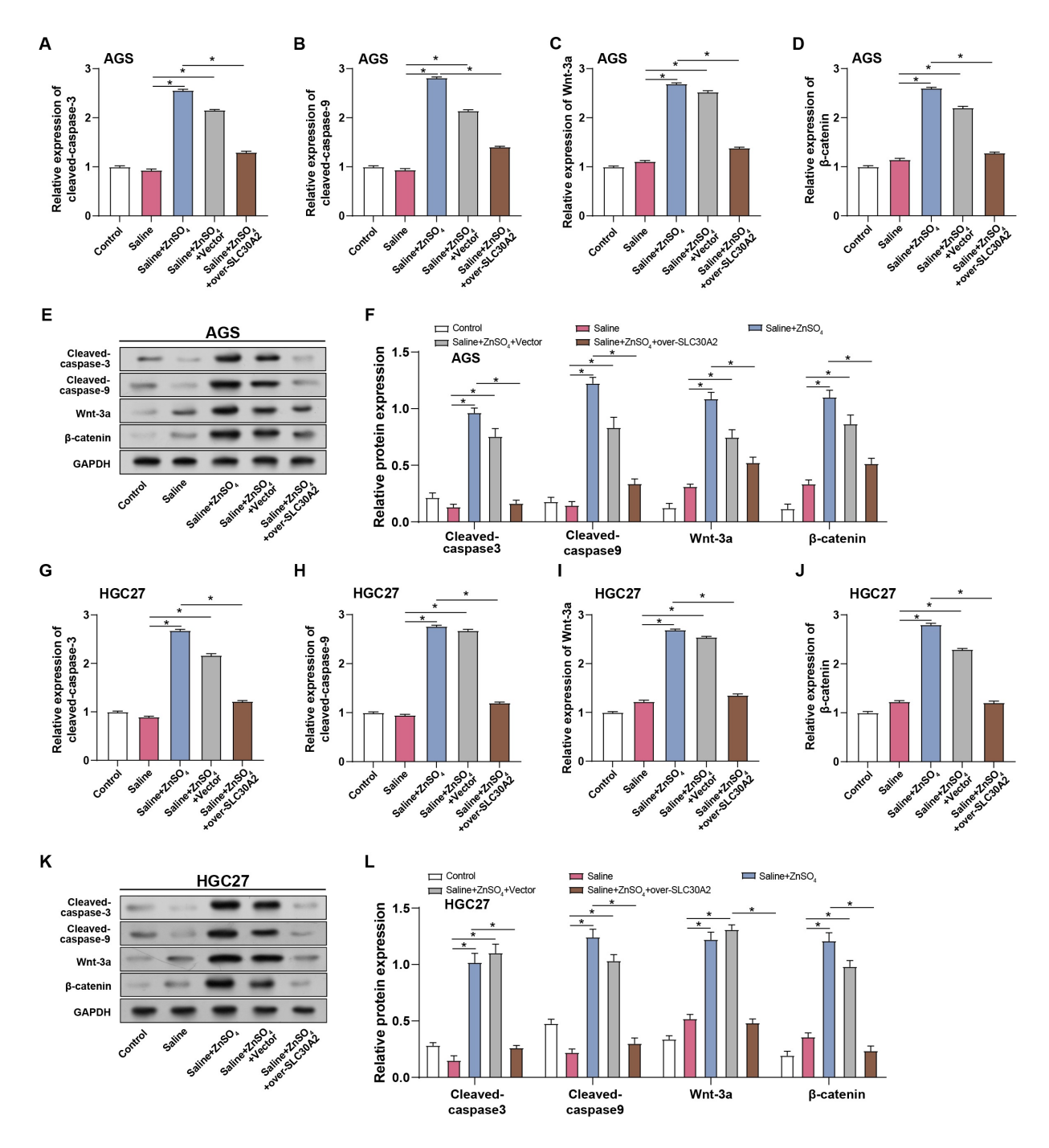


Fig. 8. Regulation of GC cell apoptosis and Wnt/ β -catenin signaling activation by ZnSO₄ and SLC30A2 overexpression. (A–F) Expression levels of Cleaved caspase-3, Cleaved caspase-9, Wnt-3a, and β -catenin in AGS cells were assessed by qRT-PCR and WB assays under different treatment conditions (control, saline, saline + ZnSO₄, saline + ZnSO₄ + Vector, and saline + ZnSO₄ + over-SLC30A2). (G–L) Expression levels of Cleaved caspase-3, Cleaved caspase-9, Wnt-3a, and β -catenin in HGC27 cells under the same treatment conditions. qRT-PCR, Quantitative real-time polymerase chain reaction; WB, Western blotting; ZnSO₄, zinc sulfate. *p < 0.05.

ence on GC pathology. To further explore the role of zinc and SLC30A2 in GC, we compared the effects of $ZnSO_4$ treatment with SLC30A2 overexpression on migration, invasion, proliferation, and apoptosis in GC cells. Our results demonstrated that SLC30A2 overexpression counteracted the $ZnSO_4$ -induced effects on migration, prolifera-

tion, invasion, and apoptosis, indicating a modulatory role of *SLC30A2* in cellular responses to zinc in GC.

Additionally, the Wnt/ β -catenin signaling pathway, which plays a crucial role in regulating genes associated with cell proliferation, differentiation, migration, and apoptosis, is implicated in this process [38,39]. Beyond these



roles, the Wnt/ β -catenin pathway is critically implicated in the control of inflammatory responses [40]. Wnt proteins attach to their receptors to initiate the pathway, which stabilizes and accumulates β -catenin [41]. After that, β catenin moves into the nucleus and starts to transcriptionally activate target genes that regulate cell destiny, proliferation, and oncogenesis [42]. Guo Q et al. [43] showed that Asymmetric dimethylarginine (ADMA) positively regulates the level of β -catenin through the Wnt/ β -catenin pathway, promoting GC cell motility and invasion and enhancing epithelial-mesenchymal transition (EMT). Additionally, research by Li L et al. [44] identified BASP1 as downregulated in GC, overexpressing BASP1 markedly reduces GC cell migration, invasion, proliferation and while enhancing apoptosis, likely via the inhibition of Wnt/ β catenin pathway activation. Our research delved into the impact of SLC30A2 overexpression on the expression of Wnt-3a and β -catenin proteins, key players in the Wnt/ β catenin signaling pathway, in GC cells exposed to ZnSO₄. We found that SLC30A2 overexpression mitigated the upregulation of these proteins induced by ZnSO₄, suggesting a role for both SLC30A2 and zinc in modulating GC cell behavior via the Wnt/ β -catenin pathway. While these findings provided valuable insights into GC pathogenesis and potential therapeutic targets, it's important to note that our experiments were confined to the cellular level and lack validation in vivo, representing a significant limitation in our study.

5. Conclusion

In summary, our study demonstrated that SLC30A2 was significantly upregulated in GC, correlating with poor prognosis. Knockdown of SLC30A2 inhibited GC cell invasion, migration, and proliferation, while promoting apoptosis and cell cycle arrest. Additionally, zinc treatment induces cytotoxicity, oxidative stress, apoptosis, and inflammatory responses in GC cells, with the Wnt/ β -catenin signaling pathway mediating these effects. Notably, overexpression of SLC30A2 attenuates zinc-induced activation, underscoring its regulatory role in GC. These findings suggested targeting SLC30A2 and zinc metabolism as a promising therapeutic strategy for GC.

Availability of Data and Materials

The datasets used and/or analyzed during the current study are available from the corresponding author upon reasonable request. The gene expression data utilized in this study originates from two publicly accessible databases: the Gene Expression Omnibus (GEO) dataset GSE54129, available at https://www.ncbi.nlm.nih.gov/gds/, and The Cancer Genome Atlas (TCGA) database's stomach adenocarcinoma (STAD) dataset, accessible at https://tcga-data.nci.nih.gov/tcga/.

Author Contributions

Conception and design of the research: FL, XHZ, and XXZ. Acquisition of data: FL, LF and XXZ. Analysis and interpretation of data: FL and XHZ. Statistical analysis: XHZ and FL. Drafting the manuscript: XXZ and LF. Revision of manuscript for important intellectual content: FL and LF. All authors contributed to editorial changes in the manuscript. All authors read and approved the final manuscript. All authors have participated sufficiently in the work and agreed to be accountable for all aspects of the work.

Ethics Approval and Consent to Participate

Not applicable.

Acknowledgment

Not applicable.

Funding

This research received no external funding.

Conflict of Interest

The authors declare no conflict of interest.

Supplementary Material

Supplementary material associated with this article can be found, in the online version, at https://doi.org/10.31083/j.fbl2910351.

References

- [1] Iwu CD, Iwu-Jaja CJ. Gastric Cancer Epidemiology: Current Trend and Future Direction. Hygiene. 2023; 3: 256–268.
- [2] Li X, Guo X, Zhu Y, Wei G, Zhang Y, Li X, et al. Single-Cell Transcriptomic Analysis Reveals BCMA CAR-T Cell Dynamics in a Patient with Refractory Primary Plasma Cell Leukemia. Molecular Therapy. 2021; 29: 645–657.
- [3] Kumar S, Patel GK, Ghoshal UC. *Helicobacter pylori*-Induced Inflammation: Possible Factors Modulating the Risk of Gastric Cancer. Pathogens. 2021; 10: 1099.
- [4] Yang L, Ying X, Liu S, Lyu G, Xu Z, Zhang X, *et al*. Gastric cancer: Epidemiology, risk factors and prevention strategies. Chinese Journal of Cancer Research. 2020; 32: 695–704.
- [5] Joshi SS, Badgwell BD. Current treatment and recent progress in gastric cancer. CA: a Cancer Journal for Clinicians. 2021; 71: 264–279.
- [6] Koustas E, Trifylli EM, Sarantis P, Papadopoulos N, Karapedi E, Aloizos G, et al. Immunotherapy as a Therapeutic Strategy for Gastrointestinal Cancer-Current Treatment Options and Future Perspectives. International Journal of Molecular Sciences. 2022; 23: 6664.
- [7] Marano L, Polom K, Patriti A, Roviello G, Falco G, Stracqualursi A, et al. Surgical management of advanced gastric cancer: An evolving issue. European Journal of Surgical Oncology. 2016; 42: 18–27.
- [8] Lin Y, Wu C, Yan W, Guo S, Liu B. Five Serum Trace Elements Associated with Risk of Cardia and Noncardia Gastric Cancer in a Matched Case-Control Study. Cancer Management and Research. 2020; 12: 4441–4451.
- [9] Zhou Y, Xu J, Luo H, Meng X, Chen M, Zhu D. Wnt signaling



- pathway in cancer immunotherapy. Cancer Letters. 2022; 525: 84–96
- [10] Yang H, Zhou H, Fu M, Xu H, Huang H, Zhong M, et al. TMEM64 aggravates the malignant phenotype of glioma by activating the Wnt/β-catenin signaling pathway. International Journal of Biological Macromolecules. 2024; 260: 129332.
- [11] Jin C, Wang T, Zhang D, Yang P, Zhang C, Peng W, et al. Acetyl-transferase NAT10 regulates the Wnt/β-catenin signaling pathway to promote colorectal cancer progression via ac⁴C acetylation of KIF23 mRNA. Journal of Experimental & Clinical Cancer Research: CR. 2022; 41: 345.
- [12] Li Z, Yang Z, Liu W, Zhu W, Yin L, Han Z, et al. Disheveled3 enhanced EMT and cancer stem-like cells properties via Wnt/βcatenin/c-Myc/SOX2 pathway in colorectal cancer. Journal of Translational Medicine. 2023; 21: 302.
- [13] Song CC, Wu LX, Chen GH, Lv WH, Chen SW, Luo Z. Six members of SLC30A/ZnTs family related with the control of zinc homeostasis: Characterization, mRNA expression and their responses to dietary ZnO nanoparticles in yellow catfish. Aquaculture. 2020; 528: 735570.
- [14] Reis BZ, Sena Evangelista KCM, Pedrosa LFC. Blood Gene Expression of Zinc Transporters as Biological Indicators of Zinc Nutrition. In Vinood BP, Victor RP (eds.) Biomarkers in Nutrition (pp. 475–493). Springer: Cham. 2022.
- [15] Ding B, Lou W, Xu L, Li R, Fan W. Analysis the prognostic values of solute carrier (SLC) family 39 genes in gastric cancer. American Journal of Translational Research. 2019; 11: 486– 498.
- [16] Guo Y, He Y. Comprehensive analysis of the expression of SLC30A family genes and prognosis in human gastric cancer. Scientific Reports. 2020; 10: 18352.
- [17] Chasapis CT, Ntoupa PSA, Spiliopoulou CA, Stefanidou ME. Recent aspects of the effects of zinc on human health. Archives of Toxicology. 2020; 94: 1443–1460.
- [18] Petryszyn P, Chapelle N, Matysiak-Budnik T. Gastric Cancer: Where Are We Heading? Digestive Diseases. 2020; 38: 280–285.
- [19] Wang T, Xu F, Lin X, Lv Y, Zhang X, Cheng W, et al. Coexposure to iron, copper, zinc, selenium and titanium is associated with the prevention of gastric precancerous lesions. Biometals. 2023; 36: 1141–1156.
- [20] Skrajnowska D, Bobrowska-Korczak B. Role of Zinc in Immune System and Anti-Cancer Defense Mechanisms. Nutrients. 2019; 11: 2273.
- [21] Rahman MM, Hossain KFB, Banik S, Sikder MT, Akter M, Bondad SEC, *et al.* Selenium and zinc protections against metal-(loids)-induced toxicity and disease manifestations: A review. Ecotoxicology and Environmental Safety. 2019; 168: 146–163.
- [22] Qi J, Xing Y, Liu Y, Wang MM, Wei X, Sui Z, et al. MCOLN1/TRPML1 finely controls oncogenic autophagy in cancer by mediating zinc influx. Autophagy. 2021; 17: 4401– 4422.
- [23] Zhu M, Zhang P, Yu S, Tang C, Wang Y, Shen Z, et al. Targeting ZFP64/GAL-1 axis promotes therapeutic effect of nabpaclitaxel and reverses immunosuppressive microenvironment in gastric cancer. Journal of Experimental & Clinical Cancer Research. 2022; 41: 14.
- [24] Fukada T, Bin BH, Hara T, Takagishi T, Yoshigai E, Lian X. Zinc transporters in physiology and pathophysiology. Essential and Toxic Trace Elements and Vitamins in Human Health (pp. 55–67). Elsevier: London. 2020.
- [25] Wessels I, Fischer HJ, Rink L. Dietary and Physiological Effects of Zinc on the Immune System. Annual Review of Nutrition. 2021; 41: 133–175.
- [26] Li Z, Liu Y, Wei R, Yong VW, Xue M. The Important Role of Zinc in Neurological Diseases. Biomolecules. 2022; 13: 28.
- [27] Oh S, Nam SK, Lee KW, Lee HS, Park Y, Kwak Y, et al. Genomic and Transcriptomic Characterization of Gastric Cancer

- with Bone Metastasis. Cancer Research and Treatment. 2024; 56: 219-237.
- [28] Ren X, Feng C, Wang Y, Chen P, Wang S, Wang J, *et al.* SLC39A10 promotes malignant phenotypes of gastric cancer cells by activating the CK2-mediated MAPK/ERK and PI3K/AKT pathways. Experimental & Molecular Medicine. 2023; 55: 1757–1769.
- [29] Silva CS, Moutinho C, Ferreira da Vinha A, Matos C. Trace minerals in human health: Iron, zinc, copper, manganese and fluorine. International Journal of Science and Research Methodology. 2019; 13: 57–80.
- [30] Cannas D, Loi E, Serra M, Firinu D, Valera P, Zavattari P. Relevance of Essential Trace Elements in Nutrition and Drinking Water for Human Health and Autoimmune Disease Risk. Nutrients. 2020; 12: 2074.
- [31] Namikawa T, Utsunomiya M, Yokota K, Munekage M, Uemura S, Maeda H, *et al.* Association between Serum Zinc Levels and Clinicopathological Characteristics in Patients with Gastric Cancer. Gastrointestinal Tumors. 2023; 10: 6–13.
- [32] Li D, Stovall DB, Wang W, Sui G. Advances of Zinc Signaling Studies in Prostate Cancer. International Journal of Molecular Sciences. 2020; 21: 667.
- [33] Gao K, Zhang Y, Niu J, Nie Z, Liu Q, Lv C. Zinc promotes cell apoptosis via activating the Wnt-3a/β-catenin signaling pathway in osteosarcoma. Journal of Orthopaedic Surgery and Research. 2020: 15: 57.
- [34] Jelić M, Mandić A, Kladar N, Sudji J, Božin B, Srdjenović B. Lipid Peroxidation, Antioxidative Defense and Level of 8hydroxy-2-deoxyguanosine in Cervical Cancer Patients. Journal of Medical Biochemistry. 2018; 37: 336–345.
- [35] Wang S, Chen Z, Zhu S, Lu H, Peng D, Soutto M, et al. PRDX2 protects against oxidative stress induced by H. pylori and promotes resistance to cisplatin in gastric cancer. Redox Biology. 2020; 28: 101319.
- [36] Lin JX, Huang YQ, Wang ZK, Xie JW, Wang JB, Lu J, et al. Prognostic importance of dynamic changes in systemic inflammatory markers for patients with gastric cancer. Journal of Surgical Oncology. 2021; 124: 282–292.
- [37] Rihawi K, Ricci AD, Rizzo A, Brocchi S, Marasco G, Pastore LV, et al. Tumor-Associated Macrophages and Inflammatory Microenvironment in Gastric Cancer: Novel Translational Implications. International Journal of Molecular Sciences. 2021; 22: 3805.
- [38] Lorzadeh S, Kohan L, Ghavami S, Azarpira N. Autophagy and the Wnt signaling pathway: A focus on Wnt/β-catenin signaling. Biochimica et Biophysica Acta. Molecular Cell Research. 2021; 1868: 118926.
- [39] A Najafi SMA. The Canonical Wnt Signaling (Wnt/β-Catenin Pathway): A Potential Target for Cancer Prevention and Therapy. Iranian Biomedical Journal. 2020; 24: 269–280.
- [40] Li X, Xiang Y, Li F, Yin C, Li B, Ke X. WNT/β-Catenin Signaling Pathway Regulating T Cell-Inflammation in the Tumor Microenvironment. Frontiers in Immunology. 2019; 10: 2293.
- [41] Colozza G, Koo BK. Wnt/β-catenin signaling: Structure, assembly and endocytosis of the signalosome. Development, Growth & Differentiation. 2021; 63: 199–218.
- [42] Pedone E, Marucci L. Role of β -Catenin Activation Levels and Fluctuations in Controlling Cell Fate. Genes. 2019; 10: 176.
- [43] Guo Q, Xu J, Huang Z, Yao Q, Chen F, Liu H, et al. ADMA mediates gastric cancer cell migration and invasion via Wnt/β-catenin signaling pathway. Clinical & Translational Oncology: Official Publication of the Federation of Spanish Oncology Societies and of the National Cancer Institute of Mexico. 2021; 23: 324.
- [44] Li L, Meng Q, Li G, Zhao L. BASP1 Suppresses Cell Growth and Metastasis through Inhibiting Wnt/β-Catenin Pathway in Gastric Cancer. BioMed Research International. 2020; 2020: 8628695.

